NIH Public Access
Author Manuscript
Curr Biol. Author manuscript; available in PMC 2009 May 25.

Published in final edited form as:
Curr Biol. 2008 November 25; 18(22): 1754–1759. doi:10.1016/j.cub.2008.09.045.

microRNA Processing Pathway Regulates Olfactory Neuron Morphogenesis

Daniela Berdnik, **Audrey P. Fan**, **Christopher J. Potter**, and **Liqun Luo***
Howard Hughes Medical Institute, Department of Biology, Stanford University, Stanford, California 94305

Summary

The micro(mi)RNA processing pathway produces miRNAs as posttranscriptional regulators of gene expression. The nuclear RNase III Drosha catalyzes the first processing step together with the dsRNA binding protein DGCR8/Pasha generating pre-miRNAs [1,2]. The next cleavage employs the cytoplasmic RNase III Dicer producing miRNA duplexes [3,4]. Finally, Argonautes are recruited with miRNAs into an RNA-induced silencing complex for mRNA recognition (Figure 1A). Here, we identify two members of the miRNA pathway, Pasha and Dicer-1, in a forward genetic screen for mutations that disrupt wiring specificity of *Drosophila* olfactory projection neurons (PNs). The olfactory system is built as discrete map of highly stereotyped neuronal connections [5,6]. Each PN targets dendrites to a specific glomerulus in the antennal lobe and projects axons stereotypically into higher brain centers [7–9]. In selected PN classes, *pasha* and *Dicer-1* mutants cause specific PN dendrite mistargeting in the antennal lobe and altered axonal terminations in higher brain centers. Furthermore, Pasha and Dicer-1 act cell-autonomously in postmitotic neurons to regulate dendrite and axon targeting during development. However, Argonaute-1 and Argonaute-2 are dispensable for PN morphogenesis. Our findings suggest a role for the miRNA processing pathway in establishing wiring specificity in the nervous system.

Results and Discussion

pasha and *Dicer-1* are required for PN dendrite morphogenesis

To identify genes that are essential for dendrite targeting in *Drosophila* olfactory projection neurons (PNs), we performed a MARCM-based mosaic forward genetic screen using novel *piggyBac* transposon insertions [10]. We uncovered the insertions *LL03660* and *LL06357*, integrated in *pasha* and *Dicer-1*, respectively (Figure 1B). Both alleles are homozygous lethal, likely to be null and referred to as $pasha^{-/-}$ and $Dicer\text{-}1^{-/-}$ mutants throughout this study. The $pasha^{-/-}$allele is an insertion in the 5′ UTR, resulting in undetectable Pasha protein in homozygous mutant neurons (Figure S1). The $Dicer\text{-}1^{-/-}$ allele is an insertion in the coding region resulting in a truncated 740 amino acid protein lacking the RNase III, PAZ and dsRNA binding domains.

The MARCM technique [11] allows us to visualize and manipulate PNs in neuroblast and single cell clones in an otherwise heterozygous animal. We use Gal4-GH146 [12] to label PNs from three neuroblast lineages, anterodorsal (ad), lateral (l), and ventral (v) PNs [7]. Wildtype

*Correspondence: lluo@stanford.edu.

Publisher's Disclaimer: This is a PDF file of an unedited manuscript that has been accepted for publication. As a service to our customers we are providing this early version of the manuscript. The manuscript will undergo copyediting, typesetting, and review of the resulting proof before it is published in its final citable form. Please note that during the production process errors may be discovered which could affect the content, and all legal disclaimers that apply to the journal pertain.

NIH-PA Author Manuscript
NIH-PA Author Manuscript
NIH-PA Author Manuscript

NIH-PA Author Manuscript

NIH-PA Author Manuscript

NIH-PA Author Manuscript

(WT) adPNs, lPNs and vPNs target stereotyped sets of glomeruli in neuroblast clones (Figure $1C_{1–3}$). *pasha*$^{-/-}$ PNs show two dendrite morphogenesis defects for all neuroblast clones. First, the dendritic density in most glomeruli is drastically reduced (compare outlined glomeruli in Figure $1C_1$ to $1D_1$ and $1C_3$ to $1D_3$). Second, dendritic branches spill into incorrect glomerular classes (arrows in Figure $1D_{1–2}$). We observed very similar PN dendritic defects in *Dicer-1*$^{-/-}$ MARCM clones. Outlined glomeruli represent a reduction in dendrites while arrows point to incorrectly innervated glomeruli (Figure $1E_{1–3}$).

We confirmed that the transposon insertions in *pasha* and *Dicer-1* are the cause for the mutant phenotype with two further experiments. First, precise excision of both transposons fully revert PN morphogenesis defects (data not shown). Second, expression of UAS-*pasha-HA* or UAS-*Dicer-1* transgenes, respectively, fully rescued *pasha* or *Dicer-1* mutant PN phenotypes in MARCM experiments (compare outlined glomeruli in Figure 1F and 1G to WT in Figure $1C_1$). Since Gal4-GH146 is expressed only in postmitotic neurons [13], these experiments also demonstrate that Pasha and Dicer-1 act in postmitotic neurons to regulate dendrite morphogenesis.

As expected, in all rescue experiments Pasha-HA localizes to the nucleus (Figure $1F_{1–2}$ and insets of Figure 2D–E) and Dicer-1 is enriched in the cytoplasm of PNs (Figure $1G_{1–2}$ and inset of Figure 2F). Endogenous Pasha protein is found ubiquitously in all cell nuclei in the brain center at 18 hours (h) after puparium formation (APF) (Figure S1A–B), when PN dendrites organize the proto-antennal lobe prior to olfactory receptor neuron (ORN) axon entry [14]. Moreover, Pasha is undetectable in *pasha*$^{-/-}$ adPNs and DL1 single neurons (yellow outlines in Figure S1 C_1–D).

Dendrite targeting in specific PN classes

To study dendrite targeting with a better resolution, we examined single-cell MARCM clones. WT DL1 single cell clones (hereafter referred to as DL1 single neurons) always target a posterior, dorsolateral glomerulus and fill the glomerulus with dendritic branches (Figure 2A). In *pasha*$^{-/-}$ PNs, 17/25 DL1 single neurons show stereotyped mistargeting defects: dendrites innervate DL1 more sparsely and also mistarget to several additional glomeruli (VA7m, VC2, VA6, DL2d, and DL5), all of which are partially innervated (arrowheads in Figure 2B). 8/25 DL1 single neurons spill their dendrites medially to adjacent glomeruli, mostly D and DL5 (data not shown). Again, *Dicer-1* single mutant neurons exhibit similar PN dendrite mistargeting although to a lower frequency. Similar stereotyped mistargeting pattern as in *pasha* mutants occur in 19/35 DL1 single neurons mutant for *Dicer-1* (arrowheads in Figure 2C), 7/35 single neurons show medially spilled dendrites and 9/35 target normally (data not shown). The variation of DL1 phenotypes could be caused by perdurance of WT protein in single cell mutant clones, which might affect Dicer-1 more than Pasha. The stereotyped DL1 targeting defect was not found in over 1400 other *piggyBac* insertions screened (unpublished), supporting the specificity of the mutant phenotype for the miRNA processing pathway.

MARCM expression of UAS-Pasha-HA in *pasha*$^{-/-}$ or UAS-Dicer-1 in *Dicer-1*$^{-/-}$DL1 single neurons fully rescued dendrite targeting (8/8 for *pasha*-HA rescue, Figure 2E; 4/4 for *Dicer-1* rescue, Figure 2F), as is the case of neuroblast clones (Figure 1F and 1G). These experiments demonstrate that Pasha and Dicer act cell-autonomously in postmitotic neurons to regulate DL1 dendrite targeting.

To expand the studies of dendrite targeting to other specific PN classes, we used Gal4-Mz19 to label fewer neurons in neuroblast clones [14]. This Gal4 line labels ~6 adPNs that innervate VA1d (asterisk) and DC3 (posterior to VA1d) in WT (Figure 2G). In 21/21 *pasha*$^{-/-}$ adPNs VA1d/DC3 is sparsely innervated and dendrites are incorrectly targeted to variable glomeruli such as DA1, VA2 and VM7 (arrowheads in Figure 2H). 23/25 *Dicer-1*$^{-/-}$ PNs show similar

NIH-PA Author Manuscript

NIH-PA Author Manuscript

NIH-PA Author Manuscript

medial mistargeting phenotypes albeit to a milder extent, innervating less distant glomeruli (arrowheads in Figure 2I). Similarly, the dendritic density is reduced and incorrect glomeruli are innervated, as in GH146 MARCM experiments (Figure 1D–E). Gal4-Mz19 is also expressed in ~7 lPNs innervating the dorsolateral DA1 glomuerlus in WT (Figure 2J). DA1 PN targeting is much less affected in *pasha* and *Dicer-1* mutants. 4/5 *pasha* mutant and 7/9 *Dicer-1* mutant lPNs target normally to DA1 with WT dendrite densities (Figure 2K–L) whereas 1/5 and 2/9 lPNs exhibit additional partial innervation of the adjacent DL3 glomerulus, respectively (data not shown). Thus, Pasha and Dicer-1 are not required equally in all PN classes, suggesting that potential miRNAs might selectively regulate the targeting of specific classes of PNs.

Pasha and Dicer-1 regulate axon terminal arborization

In addition to dendrite mistargeting, we also observed axon defects in *pasha* and *Dicer-1* mutants. WT DL1 axons project into the lateral horn (LH) via the mushroom body calyx (MBC) where they form several collateral branches. After entering the LH, DL1 axons always form one characteristic dorsal branch while the main branch terminates at the lateral edge of the LH (arrow and arrowhead, respectively, Figure 3A) [8, 9]. In *pasha* and *Dicer-1* mutant DL1 single neurons, axons extend along the normal pathway, form collaterals in the MBC, and always reach the LH. However, more than half of the mutant DL1 axons do not reach the lateral edge but stop within the LH (arrowheads in Figure 3B and 3C). The dorsal branch in the LH is either absent (arrow in Figure 3C) or reduced in length (arrow in Figure 3B). Adding one copy of a UAS-*pasha-HA* transgene in *pasha* (data not shown) or UAS-*Dicer-1* in *Dicer-1* mutant DL1 single neurons, rescued all axon phenotypes: the main branch fully extends to the lateral edge of the LH and the dorsal branch is indistinguishable from WT (arrowhead and arrow, respectively, in Figure 3D). Thus, Pasha and Dicer-1 cell-autonomously regulate PN axon terminal elaboration.

pasha mutant dendrite defects are manifested during development

To determine whether the PN dendrite targeting errors are a result of initial mistargeting, or failure to maintain stable synaptic connections later, we performed developmental studies. At 18h APF, when ORN axons have not yet entered the proto-antennal lobe [14], WT adPN, lPN (Figure $4A_{1–2}$) and vPN (not shown) dendrites have already occupied a large area of the proto-antennal lobe (encircled and labeled with N-Cadherin antibodies in red). DL1 single neurons already target their dendrites in the area of the future DL1 glomerulus (arrowhead in Figure $4A_3$). In $pasha^{-/-}$ PNs dendritic elaboration within the proto-antennal lobe is extremely reduced in all neuroblast or DL1 single cell clones at 18h APF (outlined in Figure $4B_{1–3}$). At 50h APF, glomeruli become first visible [14]. In WT adPNs, lPNs and DL1 single neurons, the same stereotyped innervation patterns as in adults are already evident even though the antennal lobe is smaller in its overall size (compare Figure $1C_{1–2}$, to $4C_{1–2}$, and 2A to $4C_3$). Dendrites of $pasha^{-/-}$PNs are reduced in density (encircled in Figure $4D_1$) and spill into lineage-inappropriate glomeruli (arrowheads in Figure $4D_{1–2}$). Moreover, stereotyped mistargeting of DL1 single neurons is already evident in 4/4 $pasha^{-/-}$ PNs at 50h APF (compare arrowheads in Figure $4D_3$ with 2B).

These data, in combination with our observation that *pasha* mutant PN dendrite phenotypes do not vary in brains of 3 and 10 days old adults (data not shown), indicate that Pasha regulates dendrite elaboration and correct targeting early during development.

Dicer-1, but not Dicer-2, is required for PN targeting

Dicer functions in small RNA maturation across species. *Dicer* mutants are defective for both transcript destruction and translational repression, suggesting that Dicer is required for the siRNA (small interfering RNA) and miRNA maturation pathway [4,15]. However, the

NIH-PA Author Manuscript

NIH-PA Author Manuscript

NIH-PA Author Manuscript

Drosophila genome contains two *Dicer* genes, *Dicer-1* and *Dicer-2*, that share similar protein domains but are different in their functions. Dicer-1 and Dicer-2 are both required for siRNA-dependent mRNA cleavage, with Dicer-2 acting in siRNA processing and Dicer-1 acting downstream of siRNA production. However, Dicer-1, but not Dicer-2, is essential for miRNA-induced silencing during translational repression [16].

To test whether the siRNA processing pathway is required for PN targeting, we made use of *Dicer-2*^{L811fsX} mutants which lack the two RNase III domains essential for dsRNA processing [16]. We found that *Dicer-2*^{L811fsX} mutant PNs exhibit normal dendrite and axon targeting (data not shown), suggesting that Dicer-2 is dispensable and the siRNA pathway is not required for PN targeting.

Next we asked whether Dicer-2 could compensate for Dicer-1's function in PN targeting since their protein domain organization is highly similar. We expressed UAS-*Dicer-2* in *Dicer-1*$^{-/-}$ PNs to test whether PN mistargeting phenotypes could be rescued as is the case for UAS-*Dicer-1* expression. We saw no alteration in the *Dicer1*$^{-/-}$ dendrite mistargeting phenotypes in DL1 PNs (compare arrowheads marking mistargeted glomuerli in Figure S2A$_1$ to S2B$_1$), adPNs, or lPNs (compare Figure S2A$_2$ to S2B$_2$ and S2A$_3$ to S2B$_3$). This observation suggests that Dicer-2 cannot replace Dicer-1's function during PN targeting. We propose that Dicer-1-dependent PN targeting defects are caused by the absence of one or several miRNA(s), because Dicer-1, but not Dicer-2, is essential for miRNA-directed translation repression and mRNA turnover.

Normal PN morphogenesis in *AGO1* and *AGO2* mutants

Many distinct mechanisms have been described for miRNA-mediated gene silencing (reviewed in [17]). However, for all these the RNA-induced silencing complex (RISC) containing the Argonaute (AGO) proteins as core components is required (Figure 1A). AGO members can be divided into two groups, the ubiquitously expressed AGO and the reproductive cell specific Piwi subfamily [18,19]. The AGO subclass containing AGO1 and AGO2 in *Drosophila* is involved in small RNA loading into the RISC. Both miRNAs and siRNAs act as components of RISCs but use different silencing mechanisms. miRNAs typically contain several mismatches when paired with target mRNAs causing mostly translational repression, whereas siRNAs are perfectly paired with target mRNAs leading to their degradation. AGO2 is described as a multiple-turnover RNA-directed RNA endonuclease acting in mRNA cleavage, whereas AGO1 functions in translational repression but also plays a role in efficient mRNA degradation [20]. However, mRNAs targeted by almost perfectly paired miRNAs can also be degraded via AGO2 [21,22]. Thus, AGO1 is typically necessary for stable miRNA maturation and essential for viability, while AGO2 is an essential component of the siRNA-directed RNA interference response [23,24].

To determine which AGO member is involved in PN targeting, we examined MARCM clones of the strong loss-of-function allele *AGO1*^{k08121} and the *AGO2*^{414} null allele [23,24]. Surprisingly, we observed normal PN dendrite and axon targeting in *AGO1*^{k08121} and *AGO2*^{414} adPNs (Figure 5A and 5C compare to WT in Figure 1C1, and data not shown), and DL1 single neurons as dendrites elaborate in the single dorsolateral DL1 glomerulus like in WT (arrowheads in Figure 5B and 5D, compare to Figure 2A). To test whether AGO1 and AGO2 could act in a redundant manner, we generated PN clones homozygous mutant for *AGO1* in an *AGO2* homozygous mutant background. 7/7 adPNs and 9/9 DL1 PNs exhibit normal targeting (Figure 5E, and arrowhead in Figure 5F). In addition, axon terminal arborization is normal in *AGO1/AGO2* mutant DL1 cells (data not shown).

There are several explanations for this surprising result. First, the *AGO1*^{k08121} allele may not be null. Second, perdurance of AGO1 protein from parental cells is capable of compensating

NIH-PA Author Manuscript

NIH-PA Author Manuscript

NIH-PA Author Manuscript

for the loss of the *AGO1* gene in homozygous mutant clones. *AGO1*^{k08121} mutants have drastically reduced mRNA levels [23], AGO1 is absent in homozygous *AGO1*^{k08121} embryo lysates and has been shown to disrupt stable miRNA maturation [24]. We also show that in *AGO1*^{k08121} mutant wing disc clones miRNA function is disrupted as in *pasha*$^{-/-}$ and *Dicer-1*$^{-/-}$ clones using a *bantam* sensor transgene (Figure S3; [25]). Because of these facts and given that WT AGO1 mRNA or protein would be heavily diluted at least in neuroblast clones, the above two explanations imply that a very small amount of AGO1 would be sufficient for PN dendrite targeting. Third, perhaps one or more members of the Piwi subfamily thought to be expressed [20] and function predominantly in the germline could compensate for the loss of AGO1/AGO2 in PNs. However, we observed normal PN morphogenesis in mutants for *piwi*^{1} [19] and *aubergine*^{LL06590} [10], both are Piwi subfamily members (data not shown). Lastly, PN dendrite targeting may utilize a novel miRNA processing mechanism that is Dicer-1-dependent but AGO-independent.

Conclusion

microRNA-mediated posttranslational regulation of gene expression has been documented in an increasing number of biological processes [26]. Many miRNAs are developmentally regulated and show tissue-specific expression. In the nervous system, miRNAs have been shown to play roles during neurogenesis, specification of neuronal fate, neuronal morphogenesis, synaptogenesis and neurodegeneration [27]. We have demonstrated a new function of the miRNA processing pathway in regulating wiring specificity of the olfactory circuit.

Our results support the model that one or more miRNA(s) are essential for regulating expression of genes that in turn regulate PN dendrite targeting and axon terminal elaboration in identified neurons during development. Candidate target genes could be transcription factors that regulate wiring specificity in postmitotic neurons, cell surface receptors for dendrite targeting, or their regulators. Expression or protein levels of such genes are essential for PN dendrite targeting [28,29]. However, each miRNA is predicted to target hundreds of mRNAs and several miRNAs can regulate one mRNA, adding much more complexity to their regulatory function [30]. Indeed, we tested 7 miRNAs with available null mutants (out of 152 miRNAs predicted in the *Drosophila* genome, see http://microrna.sanger.ac.uk/sequences); none of them exhibit PN targeting defects (Table S1). In flies, techniques that would allow the injection of individual or pools of mature miRNAs to rescue the neural phenotypes in *pasha* or *Dicer-1* mutants, or mimic these phenotypes by injecting “target protectors” that interfere with miRNA-mRNA interactions as in zebrafish [31,32], are currently not available. Therefore, it remains to be a future challenge to identify the miRNA(s), and ultimately their targets, for PN target selection. Looking for mutants with similar phenotypes as *pasha* and *Dicer-1* in forward genetic screens or candidate gene approaches may help to identify specific miRNA and their targets.

Supplementary Material

Refer to Web version on PubMed Central for supplementary material.

Acknowledgements

We thank V. Ambros, R. Carthew, S. Cohen, B. Dickson, F.-B. Gao, B. Hay, T. Uemura, and L. Zipursky for fly stocks; G. Hannon and P. Zamore for antibodies; O. Schuldiner and J. Levy for collaboration on the *piggyBac* screen; F.-B. Gao, K. Wehner, Y.-H. Chou, and O. Schuldiner for comments on the manuscript. This work was supported by fellowships from the Human Frontiers Science Program (D.B.), Damon Runyon Cancer Foundation (C.P.) and an NIH grant (R01-DC005982) to (L.L.). L.L. is a Howard Hughes Medical Institute Investigator.

NIH-PA Author Manuscript

NIH-PA Author Manuscript

NIH-PA Author Manuscript

References

1. Denli AM, Tops BB, Plasterk RH, Ketting RF, Hannon GJ. Processing of primary microRNAs by the Microprocessor complex. Nature 2004;432:231–235. [PubMed: 15531879]
2. Gregory RI, Yan KP, Amuthan G, Chendrimada T, Doratotaj B, Cooch N, Shiekhattar R. The Microprocessor complex mediates the genesis of microRNAs. Nature 2004;432:235–240. [PubMed: 15531877]
3. Hutvagner G, McLachlan J, Pasquinelli AE, Balint E, Tuschl T, Zamore PD. A cellular function for the RNA-interference enzyme Dicer in the maturation of the let-7 small temporal RNA. Science 2001;293:834–838. [PubMed: 11452083]
4. Ketting RF, Fischer SE, Bernstein E, Sijen T, Hannon GJ, Plasterk RH. Dicer functions in RNA interference and in synthesis of small RNA involved in developmental timing in C. elegans. Genes Dev 2001;15:2654–2659. [PubMed: 11641272]
5. Axel R. The molecular logic of smell. Sci Am 1995;273:154–159. [PubMed: 7481719]
6. Vosshall LB. Olfaction in Drosophila. Curr Opin Neurobiol 2000;10:498–503. [PubMed: 10981620]
7. Jefferis GSXE, Marin EC, Stocker RF, Luo L. Target neuron prespecification in the olfactory map of Drosophila. Nature 2001;414:204–208. [PubMed: 11719930]
8. Marin EC, Jefferis GSXE, Komiyama T, Zhu H, Luo L. Representation of the glomerular olfactory map in the Drosophila brain. Cell 2002;109:243–255. [PubMed: 12007410]
9. Wong AM, Wang JW, Axel R. Spatial representation of the glomerular map in the *Drosophila* protocerebrum. Cell 2002;109:229–241. [PubMed: 12007409]
10. Schuldiner O, Berdnik D, Levy JM, Wu JS, Luginbuhl D, Gontang AC, Luo L. piggyBac-based mosaic screen identifies a postmitotic function for cohesin in regulating developmental axon pruning. Dev Cell 2008;14:227–238. [PubMed: 18267091]
11. Lee T, Luo L. Mosaic analysis with a repressible cell marker for studies of gene function in neuronal morphogenesis. Neuron 1999;22:451–461. [PubMed: 10197526]
12. Stocker RF, Heimbeck G, Gendre N, de Belle JS. Neuroblast ablation in Drosophila P[GAL4] lines reveals origins of olfactory interneurons. J Neurobiol 1997;32:443–456. [PubMed: 9110257]
13. Spletter ML, Liu J, Su H, Giniger E, Komiyama T, Quake S, Luo L. Lola regulates Drosophila olfactory projection neuron identity and targeting specificity. Neural Develop 2007;2:14. [PubMed: 17634136]
14. Jefferis GS, Vyas RM, Berdnik D, Ramaekers A, Stocker RF, Tanaka NK, Ito K, Luo L. Developmental origin of wiring specificity in the olfactory system of Drosophila. Development 2004;131:117–130. [PubMed: 14645123]
15. Grishok A, Pasquinelli AE, Conte D, Li N, Parrish S, Ha I, Baillie DL, Fire A, Ruvkun G, Mello CC. Genes and mechanisms related to RNA interference regulate expression of the small temporal RNAs that control C. elegans developmental timing. Cell 2001;106:23–34. [PubMed: 11461699]
16. Lee YS, Nakahara K, Pham JW, Kim K, He Z, Sontheimer EJ, Carthew RW. Distinct roles for Drosophila Dicer-1 and Dicer-2 in the siRNA/miRNA silencing pathways. Cell 2004;117:69–81. [PubMed: 15066283]
17. Eulalio A, Huntzinger E, Izaurralde E. Getting to the root of miRNA-mediated gene silencing. Cell 2008;132:9–14. [PubMed: 18191211]
18. Hutvagner G, Simard MJ. Argonaute proteins: key players in RNA silencing. Nat Rev Mol Cell Biol 2008;9:22–32. [PubMed: 18073770]
19. Cox DN, Chao A, Baker J, Chang L, Qiao D, Lin H. A novel class of evolutionarily conserved genes defined by piwi are essential for stem cell self-renewal. Genes Dev 1998;12:3715–3727. [PubMed: 9851978]
20. Williams RW, Rubin GM. ARGONAUTE1 is required for efficient RNA interference in Drosophila embryos. Proc Natl Acad Sci U S A 2002;99:6889–6894. [PubMed: 12011447]
21. Miyoshi K, Tsukumo H, Nagami T, Siomi H, Siomi MC. Slicer function of Drosophila Argonautes and its involvement in RISC formation. Genes Dev 2005;19:2837–2848. [PubMed: 16287716]
22. Forstemann K, Horwich MD, Wee L, Tomari Y, Zamore PD. Drosophila microRNAs are sorted into functionally distinct argonaute complexes after production by dicer-1. Cell 2007;130:287–297. [PubMed: 17662943]

NIH-PA Author Manuscript

NIH-PA Author Manuscript

NIH-PA Author Manuscript

23. Kataoka Y, Takeichi M, Uemura T. Developmental roles and molecular characterization of a Drosophila homologue of Arabidopsis Argonaute1, the founder of a novel gene superfamily. Genes Cells 2001;6:313–325. [PubMed: 11318874]
24. Okamura K, Ishizuka A, Siomi H, Siomi MC. Distinct roles for Argonaute proteins in small RNA-directed RNA cleavage pathways. Genes Dev 2004;18:1655–1666. [PubMed: 15231716]
25. Brennecke J, Hipfner DR, Stark A, Russell RB, Cohen SM. bantam encodes a developmentally regulated microRNA that controls cell proliferation and regulates the proapoptotic gene hid in Drosophila. Cell 2003;113:25–36. [PubMed: 12679032]
26. Bushati N, Cohen SM. microRNA functions. Annu Rev Cell Dev Biol 2007;23:175–205. [PubMed: 17506695]
27. Gao FB. Posttranscriptional control of neuronal development by microRNA networks. Trends Neurosci 2008;31:20–26. [PubMed: 18054394]
28. Komiyama T, Luo L. Intrinsic control of precise dendritic targeting by an ensemble of transcription factors. Curr Biol 2007;17:278–285. [PubMed: 17276922]
29. Komiyama T, Sweeney LB, Schuldiner O, Garcia KC, Luo L. Graded expression of semaphorin-1a cell-autonomously directs dendritic targeting of olfactory projection neurons. Cell 2007;128:399–410. [PubMed: 17254975]
30. Chen K, Rajewsky N. The evolution of gene regulation by transcription factors and microRNAs. Nat Rev Genet 2007;8:93–103. [PubMed: 17230196]
31. Schier AF, Giraldez AJ. MicroRNA function and mechanism: insights from zebra fish. Cold Spring Harb Symp Quant Biol 2006;71:195–203. [PubMed: 17381297]
32. Choi WY, Giraldez AJ, Schier AF. Target protectors reveal dampening and balancing of Nodal agonist and antagonist by miR-430. Science 2007;318:271–274. [PubMed: 17761850]

NIH-PA Author Manuscript

NIH-PA Author Manuscript

NIH-PA Author Manuscript

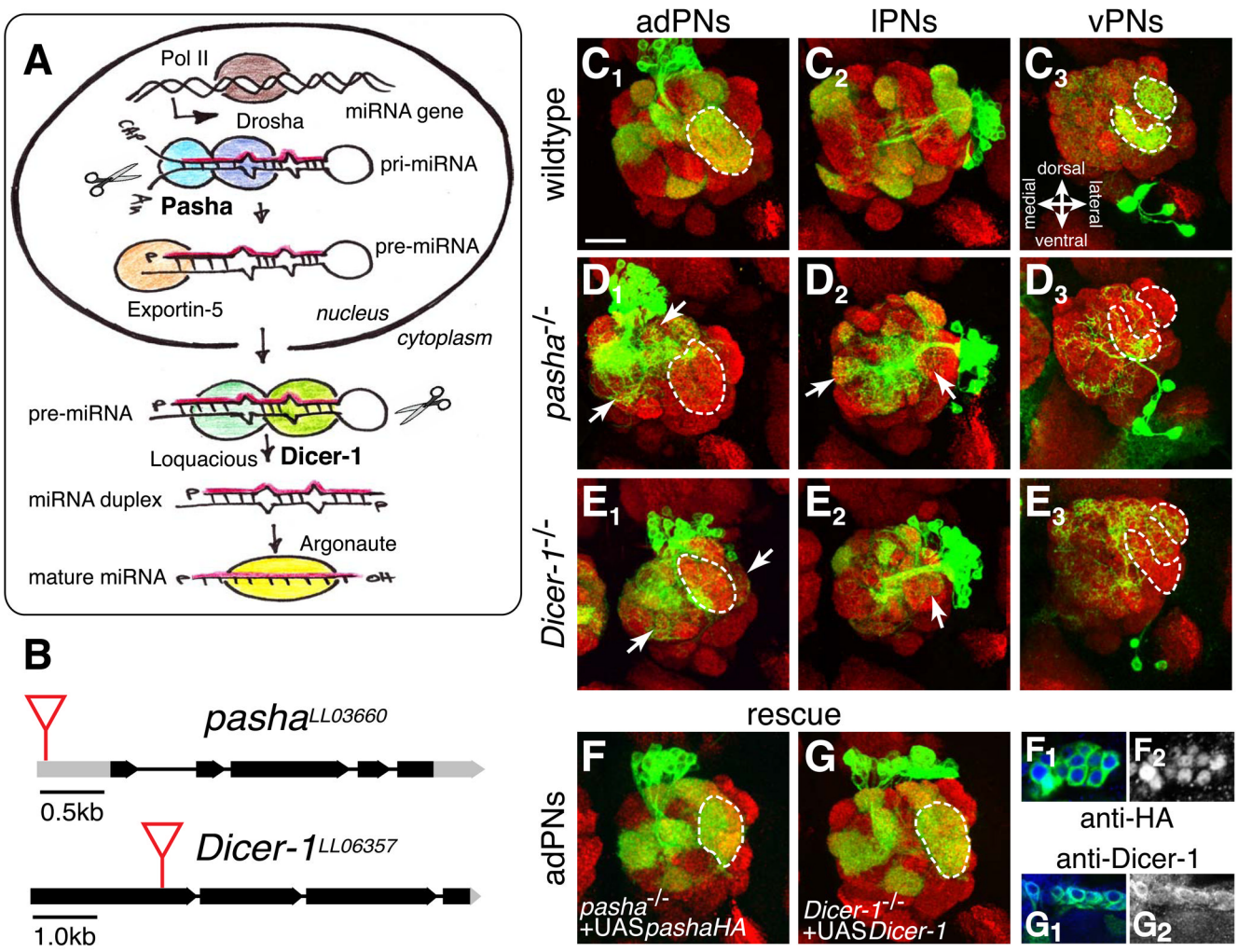

Figure 1. *pasha* and *Dicer-1* are required for dendrite targeting of olfactory projection neurons

(A) Overview of miRNA processing pathway. After transcription, pri-miRNA hairpin structures are cleaved by the RNase III enzyme Drosha into a pre-miRNA of about ~70-nt length. Drosha requires the dsRNA binding protein Pasha for this processing step in the nucleus. The pri-miRNA is exported into the cytoplasm by Exportin-5 where it is cleaved into a ~21-nt long miRNA duplex by the RNase III enzyme Dicer-1. The mature single-stranded miRNA is subsequently loaded into the Argonaute containing RNAi-induced silencing complex (RISC) that binds to complementary mRNAs to regulate translation.

(B) Genomic organization of the *pasha* and *Dicer-1* gene. Black bars represent coding and gray bars non-coding exons while the lines represents introns. Red triangles indicate the insertion sites of the *piggyBac* transposons *LL03660* and *LL06357*. The insertion in *pasha* is in the 5′UTR 515bp upstream from the start codon. The insertion in *Dicer-1* is in the first exon 2220bp 3′ of the start codon.

(C) WT adPNs (C_1), lPNs (C_2), and vPNs (C_3) target dendrites to stereotypical sets of glomeruli; VA1d and VA1lm adPNs are encircled (C_1), so are DA1 and VA1lm vPNs (C_3).

(D) *pasha*$^{-/-}$ adPNs (D_1), lPNs (D_2), and vPNs (D_3) exhibit severe dendrite targeting defects, with a general reduction in dendritic mass (compare encircled glomeruli in $1D_1$ and $1D_3$ to WT in $1C_1$and $1C_3$) and spilling of dendrites into inappropriate areas (arrows in $1D_{1–2}$).

(E) *Dicer-1*$^{-/-}$ PNs show very similar targeting defects like *pasha*$^{-/-}$ PNs.

NIH-PA Author Manuscript

NIH-PA Author Manuscript

NIH-PA Author Manuscript

(F and G) PN mutant phenotypes can be rescued completely by expressing either UAS-*pasha*-HA in *pasha*$^{-/-}$ mutant PNs (F) or UAS-*Dicer-1* in *Dicer-1*$^{-/-}$ PNs (G). Pasha-HA localizes to the nucleus (F_2), whereas Dicer-1 is enriched in the cytoplasm (G_2) of PNs.

Green is mCD8-GFP labeled MARCM clones, red is the presynaptic marker nc82, and blue is anti-HA (F_1) or anti-Dicer-1 (G_1), respectively. Scale bar represents 20μm. All images are *z*-projections of confocal stacks except in F_1, F_2, G_1, and G_2, which are single sections.

NIH-PA Author Manuscript

NIH-PA Author Manuscript

NIH-PA Author Manuscript

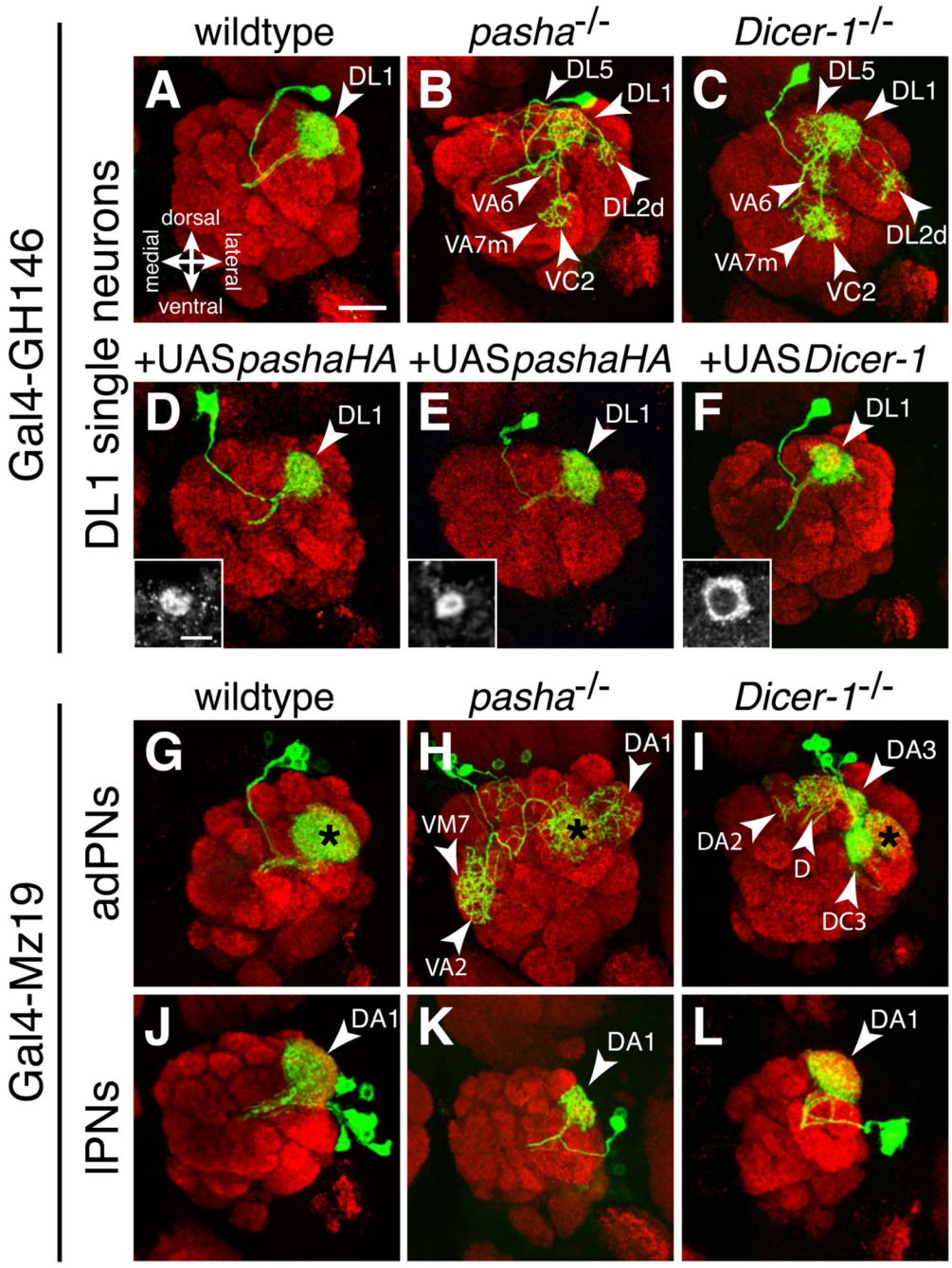

Figure 2. *pasha* and *Dicer-1* mutants cause dendrite targeting defects in specific PNs

(A) WT adPN single cell clone densely innervates DL1, a dorsolateral, posterior glomerulus (arrowhead).

(B) *pasha*$^{-/-}$ DL1 single neurons typically innervate DL1 more sparsely, and also mistarget to five additional glomeruli (VA7m, VC2, VA6, DL5, and DL2d) which are only partially innervated (arrowheads).

(C) Similar DL1 singe neuron phenotypes are seen in *Dicer-1*$^{-/-}$ PNs (arrowheads).

(D) Overexpression of Pasha-HA in WT DL1 single neurons results in normal dendrite targeting.

NIH-PA Author Manuscript

NIH-PA Author Manuscript

NIH-PA Author Manuscript

(E and F) Expressing either Pasha-HA in *pasha*$^{-/-}$ DL1 single neurons or Dicer-1 in *Dicer-1*$^{-/-}$ DL1 single neurons rescues the DL1 mistargeting phenotype completely.
(G) In WT MARCM clones, Mz19^{+} adPNs innervate the glomeruli VA1d (asterisk) and DC3 (posterior to VA1d).
(H) In *pasha*$^{-/-}$ Mz19^{+} adPNs, the dendritic mass in VA1d and DC3 is markedly reduced and additional glomeruli are innervated, such as DA1, VM7, and VA2 (arrowheads).
(I) *Dicer-1*$^{-/-}$ Mz19^{+} adPNs sparsely innervate the VA1d glomerulus and mistarget dendrites to incorrect glomeruli, such as DA3, D, and DA2 (arrowheads). The innervation pattern targeting additional glomeruli varies for *pasha*$^{-/-}$ and *Dicer1*$^{-/-}$adPNs but is always restricted to the dorsal half of the antennal lobe.
(J) In WT, Mz19^{+} lPN MARCM clones innervate a single dorsolateral glomerulus, DA1 (arrowhead).
(K) In *pasha*$^{-/-}$ and (L) *Dicer-1*$^{-/-}$ Mz19^{+} lPNs the dendritic density in DA1 is equal to WT and no additional glomeruli are innervated in most samples examined. Green is mCD8-GFP labeled PNs and their dendrites generated by MARCM using either Gal4-GH146 or -Mz19, red is the presynaptic marker nc82. Insets in (D) and (E) represent anti-HA, and in (F) anti-Dicer-1 stainings in corresponding PNs, respectively. Scale bar represents 20μm for color images and 5μm for insets in D, E, and F. Color images are *z*-projections of confocal stacks, insets are single confocal sections of cell bodies.

NIH-PA Author Manuscript
NIH-PA Author Manuscript
NIH-PA Author Manuscript

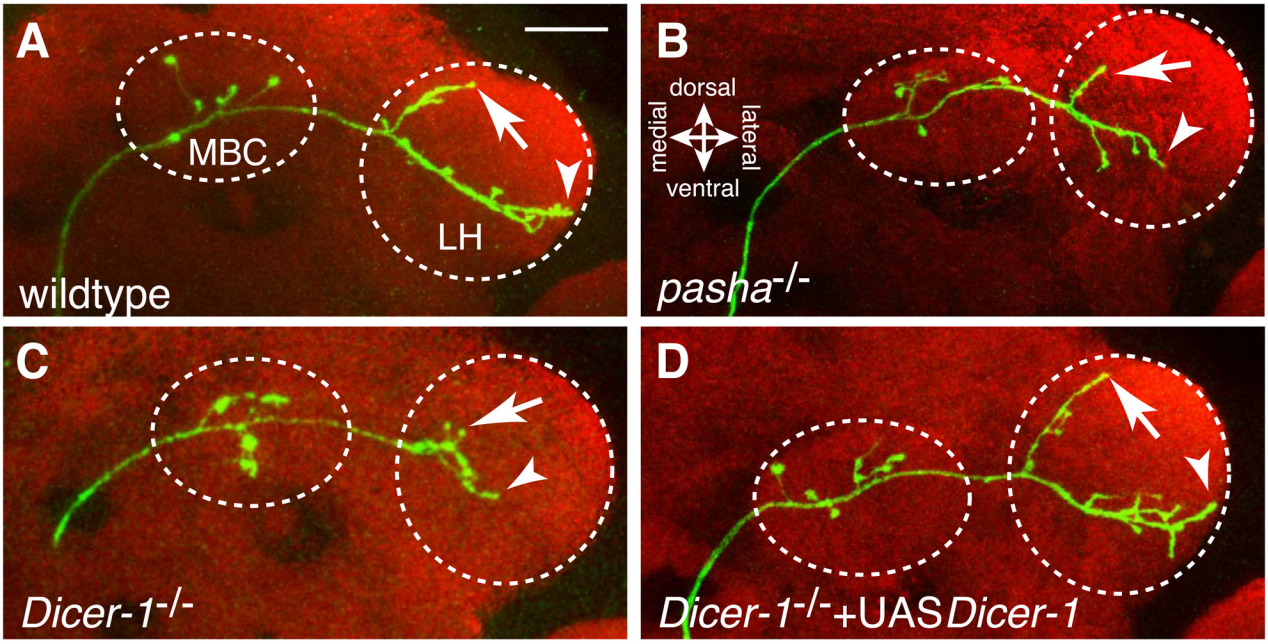

Figure 3. *Pasha* and *Dicer-1* mutants affect axon termination in the lateral horn

(A) WT DL1 PNs project their axons in a stereotypical pattern to the mushroom body calyx (MBC), where they form collateral branches, and to the lateral horn (LH) with a characteristic dorsal (arrow) and main lateral (arrowhead) branch.

(B and C) *pasha*$^{-/-}$ and *Dicer-1*$^{-/-}$ DL1 axons project into the LH but the main branches do not reach the lateral edge of the LH (arrowheads). Moreover, the dorsal branch is shorter or absent (arrow).

(D) All mutant phenotypes in axons can be fully rescued by expressing Dicer-1 in *Dicer-1*$^{-/-}$ DL1 single neurons.

Green is mCD8-GFP labeled PN axons, red is the presynaptic marker nc82. Scale bar represents 20μm. All images are *z*-projections of confocal stacks.

NIH-PA Author Manuscript
NIH-PA Author Manuscript
NIH-PA Author Manuscript

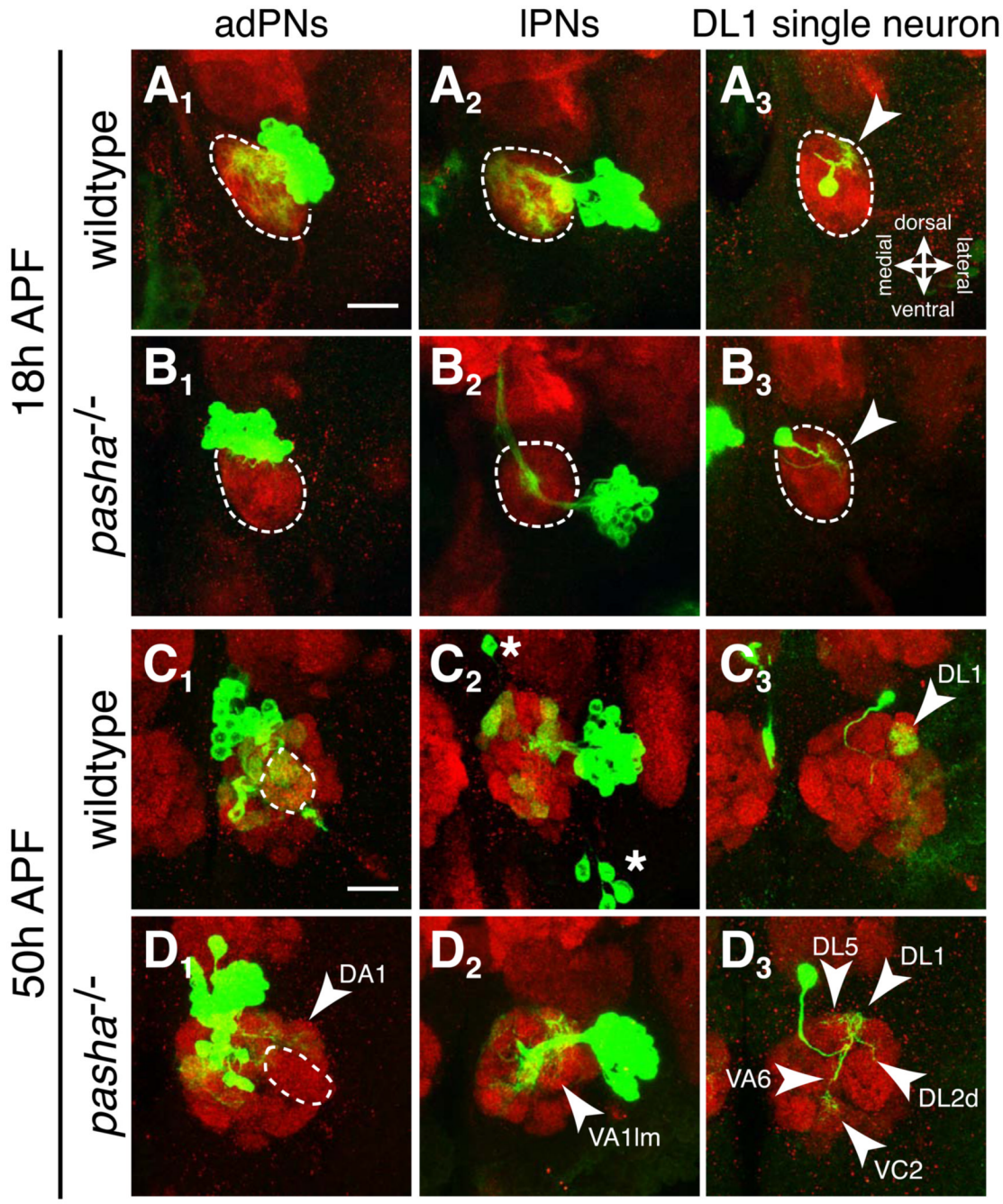

Figure 4. *pasha*$^{-/-}$ dendrite targeting defects are manifested during development

(A) WT adPNs (A_1), LPNs (A_2), and DL1 single neurons (A_3) already exhibit significant dendritic elaboration at 18 hours (h) after puparium formation (APF) in the pupal proto-antennal lobe (encircled).

(B) In *pasha*$^{-/-}$ PNs the dendritic mass is strongly reduced in adPNs (B_1) and LPNs (B_2). Dendrites of DL1 single neurons fail to elaborate on the dorsolateral area where the future DL1 glomerulus will form (compare arrowheads in A_3 to B_3).

(C) At 50h APF, WT adPNs (C_1) and LPNs (C_2) already show the stereotypic glomerular innervation of the respective lineages, VA1lm and VA1d being encircled. Dendrites of DL1 single neurons are restricted to a single, dorsolateral glomerulus (arrowhead in C_3).

NIH-PA Author Manuscript

NIH-PA Author Manuscript

NIH-PA Author Manuscript

(D) In *pasha*$^{-/-}$ adPNs and LPNs, the dendritic mass appears strongly reduced (encircled glomeruli in D_1) and dendrites target to non-specific glomeruli (arrowheads in D_{1-2}). The DL1 mistargeting phenotype to additional glomeruli like VC2, VA6, DL5, and DL2d is already manifested at 50hAPF in *pasha* mutants (arrowheads in D_3).
Note that in addition to the lPN neuroblast clones, the antennal lobe in C_2 shows vPNs and a DL1 single neuron (asterisks mark cell bodies). Their dendrites are either masked by overlaying ones in the z-stack (DL1) or weaker in intensity (vPNs).
Green is mCD8-GFP labeled MARCM clones, red is either anti-Ncadherin labeling the proto-antennal lobe at 18h APF (in A and B) or the presynaptic marker nc82 at 50h APF (in C and D). Scale bars represent 20μm. All images are *z*-projections of confocal stacks.

NIH-PA Author Manuscript
NIH-PA Author Manuscript
NIH-PA Author Manuscript

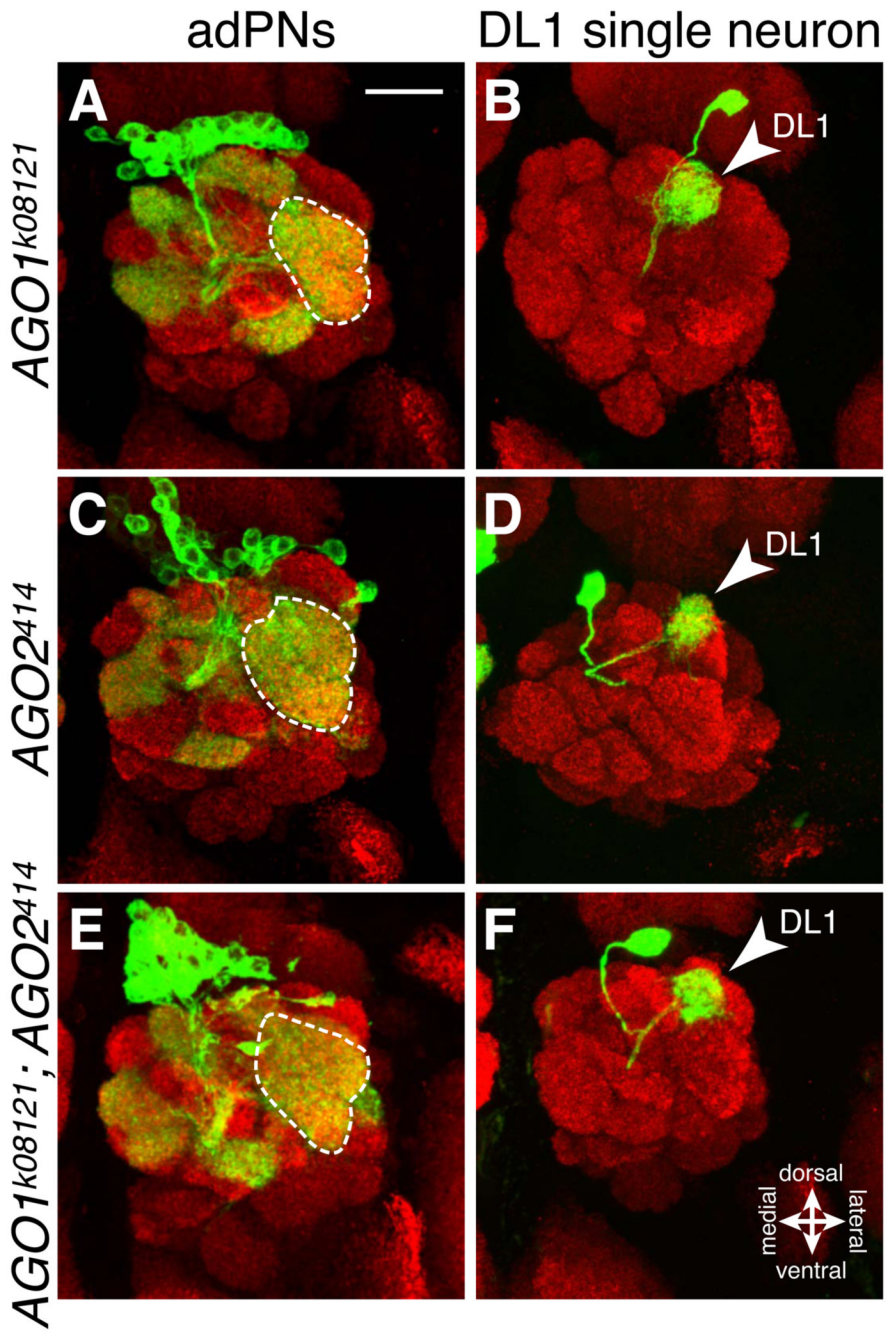

Figure 5. Normal PN dendrite targeting in the absence of AGO-1, AGO-2 or both

(A and B) *AGO1*$^{l(2)k08121}$ adPNs (VA1lm and VA1d are encircled) and DL1 single neurons (arrowhead) exhibit WT PN targeting.

(C and D) *AGO2*^{414} adPNs and DL1 single neurons target glomeruli as in WT.

(E and F) *AGO1*$^{l(2)k08121}$*; AGO2*^{414} double mutant adPNs and DL1 single neurons (arrowhead) cause no defect in glomerular target selection.

Green is mCD8-GFP labeled MARCM clones, red is the presynaptic marker nc82. Scale bar represents 20μm. All images are *z*-projections of confocal stacks.